Extracellular $CaCl_2$ was elevated to 5 mM to increase Ca^{2+} influx through the NMDA receptor. The concentration of KCl and osmolarity used were based on the minimal essential medium these neurons were cultured in. Cells were switched to this solution from Hanks balanced salt solution at least 10 min before MSCT imaging.
5. T. H. Murphy, L. A. Blatter, W. G. Wier, J. M. Baraban, *J. Neurosci.* **12**, 4834 (1992).
6. T. H. Murphy *et al.*, *ibid.* **14**, 1320 (1994).
7. L. A. Blatter and W. G. Wier, *Am. J. Physiol.* **263**, 576 (1992).
8. G. Grynkiewicz, M. Poenie, R. Y. Tsien, *J. Biol. Chem.* **260**, 3440 (1985).
9. B. Wiedermann and W. W. Franke, *Cell* **41**, 1017 (1985); D. Yoshikami and L. M. Okun, *Nature* **310**, 53 (1984). Values presented are the mean ± SD obtained from counting labeled terminals on 27 dendritic segments of five neurons for rhodamine 123 and 26 segments of four neurons for synaptophysin.
10. We used 200 μM of the racemic DL-APV. This provided a saturating concentration of the active (D) isomer to ensure complete blockade of the NMDA receptor responses. In previous studies with this preparation, we observed that this concentration did not abolish rhythmic calcium transients produced in neuronal cell bodies that are dependent on the activation of non-NMDA glutamate receptors (*13*).
11. D. M. Finch and M. B. Jackson, *Brain Res.* **518**, 269 (1990).
12. J. M. Bekkers and C. F. Stevens, *Nature* **341**, 230 (1989).
13. T. H. Murphy, J. M. Baraban, W. G. Wier, L. A. Blatter, unpublished results.
14. We calculated the frequency of MSCTs per neuron assuming an average dendritic length imaged of 200 μm per neuron and a total dendritic length of 3000 μm per neuron (estimated from three biocytin-filled neurons). MSCT frequency estimates were based on data from eight neurons used as controls in the glutamate and phorbol ester studies.
15. The probability of repeated events at a specific dendritic site was calculated with the binomial equation $P = n!/y!(n - y)![p^y(1 - p)^{n-y}]$, where y is the number of MSCTs observed at a particular site and p is the probability of an event occurring at a particular site within a single trial, assuming independent random behavior. We considered the release and action of a transmitter quantum to be equivalent to a trial (n); that is, if nine MSCTs were observed, $n = 9$. To calculate the value of p, we estimated the number of synaptic sites in a typical dendritic segment that was used for imaging studies. In these experiments, dendritic segments that averaged 205 ± 22 μm in length were imaged (images in all figures are not full frames), which contained ~80 synapses (see text). If the location at which MSCTs occurred was random, the probability of an event at any single site would be 1/80. Because it was difficult to always discriminate events occurring at adjacent synapses, we used the conservative assumption that at least thirteen 15-μm segments could be resolved in each dendrite sampled. Therefore, the probability of an event in a 15-μm segment was 0.075 (15/200).
16. J. M. Bekkers and C. F. Stevens, *Nature* **346**, 724 (1990); T. V. P. Bliss and G. L. Collingridge, *ibid.* **361**, 31 (1993); R. Robitaille and J. P. Tremblay, *Neuroscience* **40**, 571 (1991).
17. A. Malgaroli and R. W. Tsien, *Nature* **357**, 134 (1992).
18. T. Manabe, P. Renner, R. A. Nicoll, *ibid.* **355**, 50 (1992).
19. R. J. Cormier, M. D. Mauk, P. T. Kelly, *Neuron* **10**, 907 (1993); R. C. Malenka, D. V. Madison, R. A. Nicoll, *Nature* **321**, 175 (1986).
20. In experiments that exhibited more than three MSCT events, we determined the number of events at each site that showed activity for the four 10-s sampling epochs typically used. Values from different experiments were pooled, and a distribution histogram of sites with 0, 1, 2, 3, 4, 5, and 6 MSCT events was created. Data were obtained from eight separate control experiments from quiescent unstimulated cultures (n = 68 events); nine separate experiments from synaptically stimulated cultures (n = 69 events); and four separate experiments from Glu- or phorbol ester–treated cultures (n = 49 and 47 events, respectively). Expected values were calculated with the Poisson equation $P = ne^{-m}m^K/K!$, where n is the total number of presumed sites (assumed to be 13 for each experiment), m is the mean number of events per site, and K is the number of events 0 to 6. The observed values were not significantly different from the expected distribution for unstimulated cultures, as indicated by χ^2 analysis ($\alpha > 0.1$); however, expected values (for synaptically stimulated cultures and cultures stimulated with Glu or phorbol ester) were significantly different from those observed ($\alpha < 0.025$).
21. W. G. Regehr and D. W. Tank, *Nature* **345**, 807 (1990).
22. W. Muller and J. A. Connor, *ibid.* **354**, 73 (1991).
23. P. B. Guthrie, M. Segal, S. B. Kater, *ibid.*, p. 76.
24. C. Koch and A. Zador, *J. Neurosci.* **13**, 413 (1993).
25. D. G. Amaral, N. Ishizuka, B. Claiborne, *Prog. Brain Res.* **83**, 1 (1990).
26. C. Rosenmund, J. D. Clements, G. L. Westbrook, *Science* **262**, 754 (1993); N. A. Hessler, A. M. Shirke, R. Malinow, *Nature* **366**, 6455 (1993).
27. Supported by grants from the USPHS and the American Heart Association, Maryland affiliate. We thank D. Rodgers for secretarial assistance and D. Linden, D. Yue, D. Blake, and L. Raymond for helpful comments.

4 October 1993; accepted 7 December 1993

Locally Distributed Synaptic Potentiation in the Hippocampus

Erin M. Schuman*† and Daniel V. Madison

The long-lasting increase in synaptic strength known as long-term potentiation has been advanced as a potential physiological mechanism for many forms of both developmental and adult neuronal plasticity. In many models of plasticity, intercellular communication has been proposed to account for observations in which simultaneously active neurons are strengthened together. The data presented here indicate that long-term potentiation can be communicated between synapses on neighboring neurons by means of a diffusible messenger. This distributed potentiation provides a mechanism for the cooperative strengthening of proximal synapses and may underlie a variety of plastic processes in the nervous system.

Most models of neuronal development, learning, memory, and circuit reorganization include alterations of the strength of synaptic connections between neurons. These models suggest that communication occurs between like synapses, such that synapses that are coactive tend to function as a group (*1*). Long-term potentiation (LTP), the long-lasting increase in synaptic transmission that is induced by intense synaptic activity (*2*), has been advanced as a potential physiological mechanism for these forms of plasticity. Although LTP clearly results in enhanced synaptic transmission, it is less clear whether it possesses the properties necessary to mediate the intercellular communication inherent in most models of coactive strengthening. When LTP is selectively induced in one synaptic pathway, other synaptic inputs to the same cell do not undergo LTP (*3*). This input specificity has usually been interpreted to mean that potentiation cannot be communicated from one synapse to another.

During the induction of LTP, postsynaptic events such as *N*-methyl-D-aspartate (NMDA) receptor activation and Ca^{2+} influx have been suggested to lead to the generation of different diffusible signals (*4*), such as arachidonic acid (*5*), carbon monoxide (*6*), nitric oxide (NO) (*7–9*), and platelet-activating factor (*10, 11*). These signals have been proposed to mediate the synaptic enhancement of LTP (*5–13*). In theory, a diffusible messenger could act in a strictly retrograde manner, influencing only the synapses where it is generated, or it could diffuse to enhance the synapses of nearby neurons as well. Indeed, an LTP induction procedure, pairing postsynaptic depolarization of a single neuron with low-frequency stimulation of afferent fibers (*14*) decreases the action potential latency in both the depolarized cell as well as nearby cells (*15, 16*).

To examine whether long-lasting synaptic potentiation could spread to nearby synapses in hippocampal slices, we made simultaneous intracellular recordings from two nearby CA1 pyramidal neurons and monitored the excitatory postsynaptic potentials (EPSPs) resulting from stimulation of Schaffer collaterals (*17*) (Fig. 1A). We detected no synaptic or electrical coupling

Department of Molecular and Cellular Physiology, Beckman Center for Molecular and Genetic Medicine, Stanford Medical School, Stanford, CA 94305.

*Present address: Division of Biology 216-76, California Institute of Technology, Pasadena, CA 91125.
†To whom correspondence should be addressed.

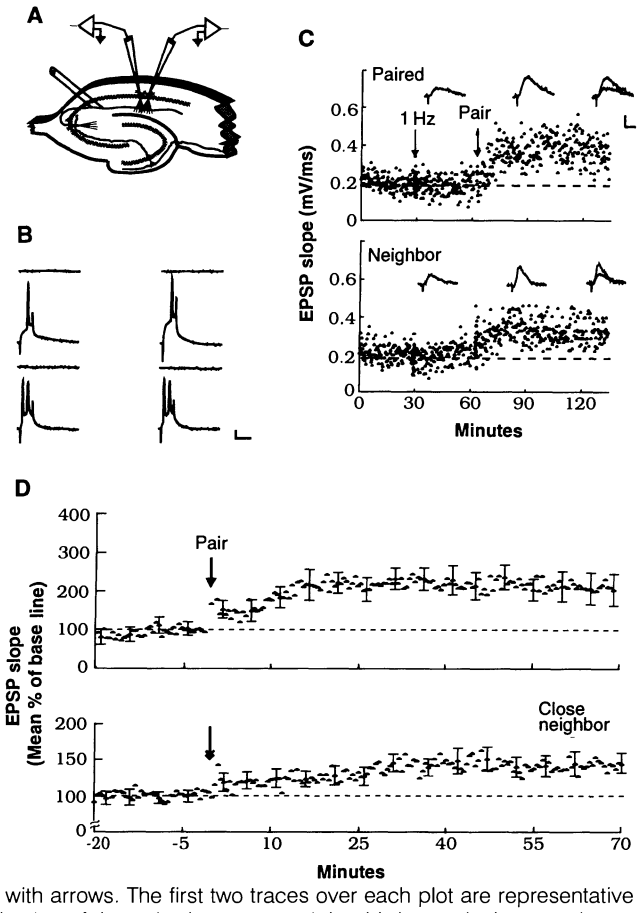

Fig. 1. Demonstration of distributed synaptic potentiation. (**A**) Diagram of the position of stimulating and recording electrodes in the hippocampal slice preparation. Two nearby CA1 pyramidal cells were impaled, and the excitatory responses were recorded to test shocks delivered to the Schaffer collaterals by a bipolar stimulating electrode. (**B**) Electrophysiological traces testing for electrical or synaptic connectivity between the cells shown in (C). Shown are action potentials elicited by depolarizing current injection into the paired cell (top) and neighboring cell (bottom) before (left) and after (right) LTP induction; above each action potential is the corresponding trace of the other cell. Scale bar: 15 mV, 50 ms. (**C**) EPSP slope from a single paired (top) and neighboring (bottom) neuron [same pair as in (B)]. Low-frequency stimulation (1 Hz) and low-frequency stimulation paired with depolarization (Pair) are indicated with arrows. The first two traces over each plot are representative EPSPs before and after LTP induction of the paired neuron, and the third trace is the superimposition of the two. Scale bar: 10 mV, 10 ms. (**D**) Ensemble average for EPSP slope measurements from paired (top) and close neighbor (bottom) neurons before and after LTP induction in the paired neuron (n = 20).

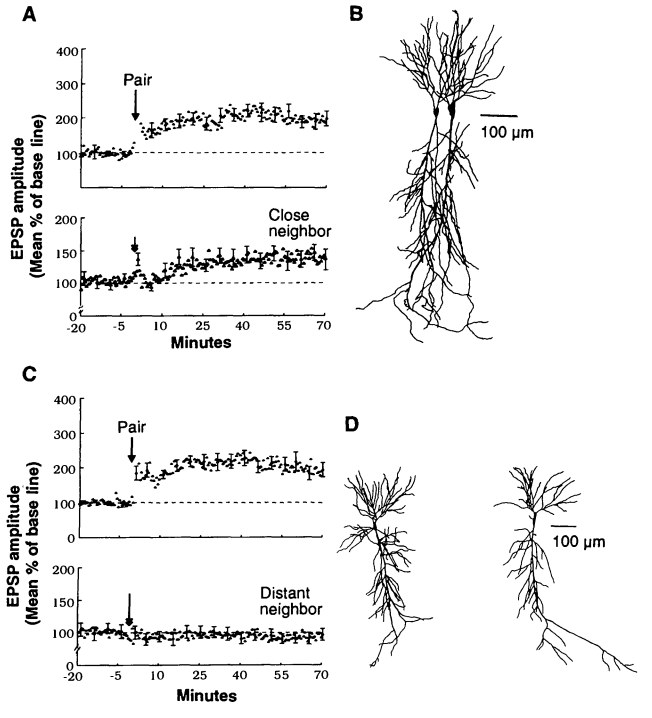

Fig. 2. (**A**) Ensemble averages of EPSP amplitudes for nearby pyramidal neurons (n = 20). Average data for the paired neurons (top) and neighboring neurons (bottom) in response to LTP induction in the paired neuron. The mean pre-LTP EPSP amplitudes for paired and neighboring cells were 9.4 ± 0.9 mV and 8.0 ± 0.6 mV, respectively. (**B**) Camera lucida tracing of a pair of biocytin-filled neurons from (A). (**C**) Ensemble averages for dual intracellular recordings from distant (~500 μM) CA1 pyramidal neurons (n = 17). Average EPSP amplitude data for the paired neurons (top) and distant neighbor neurons (bottom) before and after LTP induction in the paired neuron. The mean pre-LTP EPSP amplitudes for paired and neighboring cells were 8.5 ± 0.6 mV and 7.3 ± 0.7 mV, respectively. (**D**) Camera lucida tracing of biocytin-filled neurons from (C).

between any pairs of CA1 neurons before or after LTP induction (Fig. 1B). After establishing a base line of synaptic transmission, we stimulated the presynaptic axons at a low frequency (1 Hz, 30 to 45 s). As previously documented (*15, 17*), this brief low-frequency stimulation had no long-lasting effect on synaptic transmission (Fig. 1C), although in many experiments we observed a transient (~5 to 10 min) depression of synaptic responses. We then induced LTP in one cell (the "paired" cell) by pairing postsynaptic depolarization (to 0 mV) with the low-frequency stimulation (1 Hz, 30 to 45 s) (Fig. 1C).

If the induction of LTP in the paired cell results in the production of a diffusible signal, then this signal might also influence synaptic transmission at nearby cell synapses. Indeed, the synapses onto the neighboring cell also developed potentiated responses after LTP induction in the paired cell (Fig. 1C). Because no change in synaptic transmission occurred after 1-Hz stimulation alone, but only when the paired cell was also depolarized, the enhancement of synaptic strength observed in neighboring cell synapses must be a result of LTP induction in the paired cell. The ensemble averages (*18*) of the EPSP slope and amplitude for all 20 experiments are shown in Figs. 1D and 2A. The paired neurons exhibited increases in synaptic strength that were on average 183.8 ± 15.0% and 187.1 ± 18.3% of base line values for EPSP slope and amplitude measurements, respectively (mean percent of base line 1 hour after LTP induction ± SEM, n = 20). Of the 20 paired neurons tested, 17 exhibited potentiation that was at least 130% of base line levels, with individual values for all 20 cells ranging from no potentiation to 330%. The neighboring neurons exhibited an average enhancement of 137.5 ± 11.0% (slope) and 129.3 ± 9.1% (amplitude) of base line transmission levels (Figs. 1D and 2A). Sixteen of the neighboring neurons exhibited potentiation that was at least 115% of base line levels, with individual values for all 20 cells ranging from no potentiation to 253%. These results demonstrate that LTP induction in a single CA1 pyramidal cell can augment synaptic strength at connections onto neighboring neurons.

To ascertain the distance between the neurons, in several experiments we included biocytin (1%) in the recording electrodes and filled each pyramidal neuron during the experiment (*19*). The cell bodies of the example in Fig. 2B were ~38.0 μm apart, and the dendritic arbors of the two neurons overlapped extensively. The mean distance between CA1 cell somata for the experiments in which we included biocytin in our electrodes was 142.1 ± 36.1 μm (range: 20.0 to 285.0 μm, n = 9). In all

cases, it appeared that the dendritic fields of the two stained neurons were intertwined.

We directly assessed the spatial limits of the synaptic enhancement by conducting similar electrophysiological experiments from pairs of CA1 pyramidal neurons that were spatially remote from one another (~500 μm). As above, induction of LTP in the paired neuron significantly increased synaptic strength (173.6 ± 10.7%, n = 17) (Fig. 2C). In contrast, the synapses onto the "distant" neighbor did not exhibit any potentiation (97.8 ± 8.6%) (Fig. 2C). A camera lucida reconstruction of a representative pair of distant pyramidal neurons that are ~585 μm apart is shown in Fig. 2D. On average, the cell bodies of the distant pyramidal cells were 595.0 ± 58.8 μm apart (range: 340 to 800 μm, n = 7). None of these neuron pairs had regions of detectable dendritic overlap. There was a significant negative correlation between the distance between the pyramidal cell bodies and the magnitude of the potentiation exhibited at the neighboring cell synapses (n = 16) (Spearman's rank correlation = −0.58, P < 0.05). Thus, the distributed synaptic enhancement is spatially restricted, occurring only when neurons are close to one another.

To examine the contribution of putative diffusible signals, we introduced the NO synthase inhibitor *N*-methyl-L-arginine (L-Me-Arg) into the paired neuron to block the postsynaptic generation of NO. As reported [(7, 8) but see (9)], postsynaptic injection of L-Me-Arg into the paired cell prevented long-lasting synaptic potentiation at its own synapses (99.8 ± 6.9%) (Fig. 3A). The injection of L-Me-Arg into the paired cell also prevented the enhancement of synaptic strength at neighboring cell synapses (102.2 ± 10.1%) (Fig. 3A). Camera lucida reconstructions (Fig. 3B) revealed that the mean distance between pairs of pyramidal neurons in these experiments was statistically indistinguishable from the distance between the pairs of neurons that compose the near group (x = 143.3 ± 43.6 μm, n = 7). This finding suggests that NO production in the paired cell is required for the enhancement of synaptic transmission at the neighboring cell synapses. While these results are consistent with the idea that NO itself may be responsible for the neighboring synapse potentiation, at present we cannot rule out the possibility that a process downstream from the production of NO is responsible.

In a few experiments, we held both intracellular recordings long enough to subsequently assess whether inducing LTP in the neighboring cell could produce any enhancement at synapses onto the NO synthase (NOS)–inhibited neuron. In three of five cases, pairing depolarization of the neighboring cell with low-frequency stimulation enhanced synaptic strength at synapses onto the NOS-inhibited neuron. Consistent with this finding, we found that although postsynaptic injections of NOS inhibitors prevented LTP induced by pairing depolarization with low-frequency stimulation (109.5 ± 4.5%, n = 15) (Fig. 4A), high-frequency stimulation of the same afferent pathway enhanced synaptic transmission at the synapses onto the NOS-inhibited cell (159.3 ± 19.7%, n = 15) (Fig. 4A). This suggests that neighboring cells that become depolarized and undergo LTP induction during tetanic stimulation may produce NO that diffuses to influence the synapses onto the inhibited neuron (Fig. 4B). This interpretation is reinforced by the demonstration that high-frequency stimulation in the presence of an extracellularly applied NOS inhibitor (which presumably acts on all pyramidal neurons) does not potentiate either the extracellular field (7, 8) or intracellular EPSP (90.5 ± 5.9, n = 4).

The simplest interpretation of the above result is that LTP induction in neighboring neurons can compensate for a disruption of LTP induction mechanisms in a nearby pyramidal cell. However, individual postsynaptic injections of Ca^{2+} chelators (20)

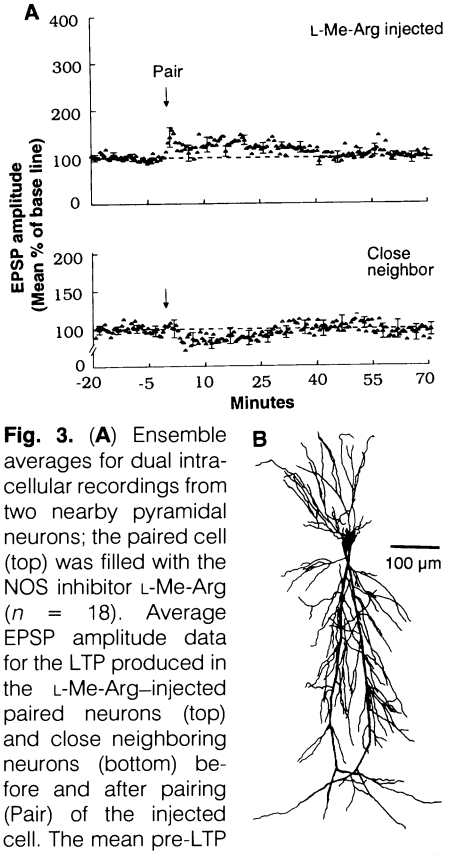

Fig. 3. (**A**) Ensemble averages for dual intracellular recordings from two nearby pyramidal neurons; the paired cell (top) was filled with the NOS inhibitor L-Me-Arg (n = 18). Average EPSP amplitude data for the LTP produced in the L-Me-Arg–injected paired neurons (top) and close neighboring neurons (bottom) before and after pairing (Pair) of the injected cell. The mean pre-LTP EPSP amplitudes for paired and neighboring cells were 8.6 ± 0.8 mV and 8.0 ± 0.6 mV, respectively. (**B**) Camera lucida tracing of two biocytin-filled neurons (A). In the example shown, cell bodies are within 10 μm of each other.

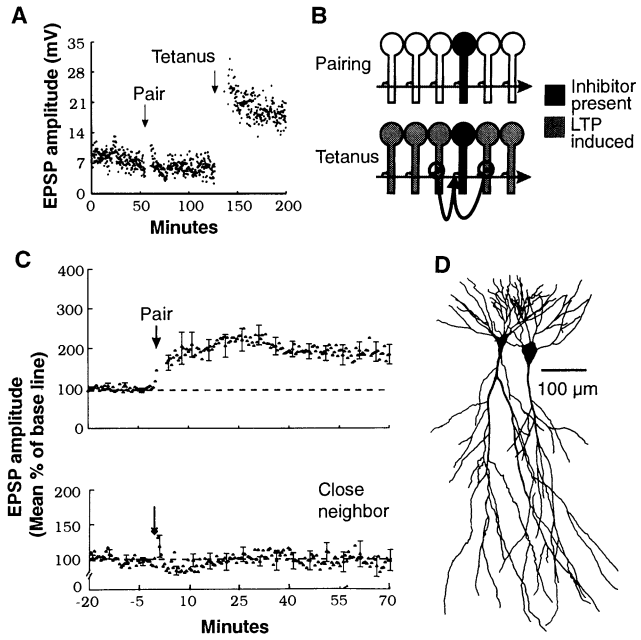

Fig. 4. Representative experiment to examine the potential contribution of neighboring synapses to LTP induced at synapses onto an NOS-inhibited pyramidal neuron. (**A**) EPSP amplitude from a single CA1 pyramidal neuron filled with the NOS inhibitor L-Me-Arg. (**B**) Diagram depicting how neighboring neurons may provide NO to induce LTP onto an NOS-inhibited neuron during LTP induction. Tetanic stimulation delivered to afferent fibers should induce LTP in many neurons. During tetanic stimulation, the NO produced in the neighboring neurons may diffuse to potentiate synapses onto the NOS-inhibited neuron. (**C**) Ensemble averages for dual recordings from two nearby pyramidal neurons (n = 14). A standard intracellular micropipette was used to record from the paired cell, and the neighboring cell (bottom) was recorded from in whole-cell voltage-clamp mode and filled with the Ca^{2+} chelator BAPTA. During the induction of LTP in the paired cell, the neighboring neuron was hyperpolarized to −95 mV. Top plot shows average data for the LTP produced by pairing (Pair). Bottom plot shows average data for the enhancement observed in the neighboring neuron in response to LTP induction in the paired neuron. The mean pre-LTP EPSP and EPSC amplitudes were 8.4 ± 1.0 mV and 93.5 ± 13.5 pA, respectively. (**D**) Camera lucida tracing of biocytin-filled neurons. In the example shown, cell bodies are within 65 μm of each other.

or membrane hyperpolarization (*21*) can prevent LTP induced by tetanic stimulation, indicating that this simple interpretation cannot be correct. Therefore, we assessed the possibility that postsynaptic Ca^{2+} or alterations in the membrane potential of the neighboring postsynaptic cell may be required for the distributed synaptic enhancement by recording from neighboring neurons in the whole-cell voltage-clamp mode with pipettes containing the Ca^{2+} chelator BAPTA (10 mM). To further compromise the neighboring neuron, we whole-cell dialyzed it for at least 40 min before the experiment. Also, during LTP induction of the paired neuron, the neighboring cell was voltage-clamped at −95 mV. As above, paired neurons exhibited significant potentiation (193.8 ± 26.3%, n = 14) (Fig. 4C). However, the combination of postsynaptic dialysis, Ca^{2+} chelation, and hyperpolarization abolished the neighboring cell enhancement (97.6 ± 14.4%) (Fig. 4C). The pairs of neurons used in these experiments were anatomically close (x = 79.4 ± 21.6 μm) (Fig. 4D), indicating that the neighboring neurons should have exhibited synaptic enhancement. The inability of the neighboring neuron to exhibit synaptic potentiation under these conditions suggests that the postsynaptic neighboring neuron may actively participate in the enhancement.

These results are consistent with the synapse specificity that has been reported for LTP in which no spreading of potentiation is observed between two independent afferent pathways that converge on the same postsynaptic neuron (*3*). The distributed potentiation we have described may be limited by two factors: (i) the presence or absence of synaptic activity and (ii) the proximity of the paired and neighbor synapses. In all of the experiments we have described, both the neighboring and the paired neurons received synaptic input from a common set of afferent fibers; thus, both sets of synapses were active during LTP induction. However, it is clear that low-frequency synaptic activity is not sufficient to produce enhancement, because 1-Hz stimulation did not increase synaptic strength at neighboring cell synapses. Thus, the presence of synaptic activity may work in concert with other factors generated in paired neurons. Our results do indicate spatial constraints on the spreading of synaptic enhancement: synapses onto distant neighbor cells were not potentiated, despite receiving the same synaptic input as paired cells.

The demonstration that LTP induction in a single CA1 pyramidal neuron can potentiate synaptic transmission at neighboring cell synapses implies the existence of a diffusible signal generated in paired neurons during LTP induction. Our results suggest that NO production is important for this phenomenon. In addition, we observed that the blockade of LTP produced by postsynaptic injections of NOS inhibitors can be overcome by LTP induction in neighboring cells. Taken together, these two results suggest that during LTP induction NO may diffuse to increase synaptic strength at nearby synapses.

Our data do not indicate whether the enhancement of synaptic transmission at neighboring synapses is mediated by pre- or postsynaptic mechanisms. However, the combination of postsynaptic dialysis, Ca^{2+} chelators, and hyperpolarization of the neighboring cell prevented the enhancement, suggesting that the postsynaptic neighboring cell plays an active role. There are two general possibilities to account for a distributed LTP that requires involvement of the postsynaptic cell for its induction. First, the distributed potentiation could be both induced and expressed by postsynaptic mechanisms in the receiving cell: A single messenger produced in the paired cell could diffuse to the neighboring neuron and interact with a Ca^{2+}- or voltage-dependent postsynaptic target to bring about the enhancement. Second, the distributed potentiation could be expressed by changes in the presynaptic side of the receiving synapse, but require a postsynaptic contribution dependent on Ca^{2+} or voltage or both. This contribution could be either a constitutive or stimulated process. As one example of a constitutive process, intracellular Ca^{2+} activity, resulting from the tonic stimulation of postsynaptic NMDA channels (*22*) or window currents through voltage-dependent Ca^{2+} channels, might support the release of a local retrograde messenger that is permissive for distributed potentiation. Alternatively, the local messenger may be stimulated by depolarization arising from either the 1-Hz stimulation or increases in extracellular K^+ produced during depolarization of the paired cell (*23*). According to both of these ideas, both the signal generated in the paired neuron during LTP induction and the Ca^{2+} or voltage-dependent signal produced in the neighboring cell would be required for the expression of enhancement in the neighboring cell.

Thus, the formation of synaptic changes previously thought to be restricted to synapses onto a single cell can also result in synaptic changes at nearby synapses. As such, diffusible signals proposed to act as retrograde synaptic signals may serve an alternate function of amplifying synaptic transmission at active synapses close to the site of messenger generation. During development, this locally distributed potentiation may participate in the formation of functionally segregated anatomical structures such as cortical columns (*15, 24*) and could also induce temporary functional domains in regions where no such anatomical specialization exists. This type of enhancement may also serve to locally amplify synaptic signals that underlie common neuronal functions.

REFERENCES AND NOTES

1. E. R. Kandel and T. J. O'Dell, *Science* **258**, 243 (1992); C. S. Goodman and C. J. Shatz, *Neuron* **10**, 77 (1993).
2. T. V. P. Bliss and T. Lomo, *J. Physiol. (London)* **232**, 331 (1973).
3. P. Andersen, S. H. Sundberg, O. Sveen, H. Wigstrom, *Nature* **266**, 736 (1977); G. Lynch, T. Dunwiddie, V. Gribkoff, *ibid.*, p. 737.
4. T. V. P. Bliss, R. M. Douglas, M. L. Errington, M. A. Lynch, *J. Physiol. (London)* **377**, 391 (1986); J. A. Gally, P. R. Montague, G. N. Reeke, G. M. Edelman, *Proc. Natl. Acad. Sci. U.S.A.* **87**, 3547 (1990).
5. J. H. Williams, J. L. Errington, T. V. P. Bliss, *Nature* **341**, 739 (1989).
6. M. Zhuo, S. A. Small, E. R. Kandel, R. D. Hawkins, *Science* **260**, 1946 (1993), C. F. Stevens and Y. Y. Wang, *Nature* **364**, 147 (1993).
7. E. M. Schuman and D. V. Madison, *Science* **254**, 1503 (1991); T. J. O'Dell, R. D. Hawkins, E. R. Kandel, O. Arancio, *Proc. Natl. Acad. Sci. U.S.A.* **88**, 11285 (1991).
8. G. A. Bohme, C. Bon, J. M. Stutzmann, A. Doble, J. C. Blanchard, *Eur. J. Pharmacol.* **199**, 379 (1991); J. E. Haley, G. L. Wilcox, P. F. Chapman, *Neuron* **8**, 211 (1992).
9. Recent studies [V. K. Gribkoff and J. T. Lum-Ragan, *J. Neurophysiol. (London)* **68**, 639 (1992); Y. Izumi, D. B. Clifford, C. F. Zorumski, *Science* **257**, 1273 (1992); D. M. Chetkovich, E. Klann, J. D. Sweatt, *Neuroreport* **4**, 919 (1993); J. E. Haley, P. L. Malen, P. F. Chapman, *Neurosci. Lett.* **160**, 85 (1993); J. H. Williams, Y. G. Li, M. L. Errington, K. Murphy, T. V. P. Bliss, *Neuron* **11**, 877 (1993)] have reported that NOS inhibitors do not block LTP under all experimental conditions.
10. G. D. Clark, L. T. Happel, C. F. Zorumski, N. G. Bazan, *Neuron* **9**, 1211 (1992).
11. A. Arai and G. Lynch, *Eur. J. Neurosci.* **4**, 411 (1992); A. Wieraszko, G. Li, E. Kornecki, M. V. Hogan, Y. H. Ehrlich, *Neuron* **10**, 553 (1993).
12. I. Herrero, M. T. Miras-Portugal, J. Sanchez-Prieto, *Nature* **360**, 163 (1992).
13. B. Miller, M. Sarantis, S. F. Traynelis, D. Atwell, *ibid.* **355**, 722 (1992).
14. B. Gustafsson, H. Wigstrom, W. C. Abraham, Y. Y. Huang, *J. Neurosci.* **7**, 774 (1987).
15. T. Bonhoeffer, V. Staiger, A. Aertsen, *Proc. Natl. Acad. Sci. U.S.A.* **86**, 8113 (1989).
16. A. Kossel, T. Bonhoeffer, J. Bolz, *Neuroreport* **1**, 115 (1990).
17. Hippocampal slices were prepared as described [D. V. Madison and R. A. Nicoll, *J. Physiol. (London)* **398**, 123 (1986)]. Hippocampal slices were submerged in a stream of solution containing 119 mM NaCl, 2.5 mM KCl, 1.3 mM $MgSO_4$, 2.5 mM $CaCl_2$, 1.0 mM NaH_2PO_4, 26.2 mM $NaHCO_3$, and 11.0 mM glucose. Artificial cerebrospinal fluid was maintained at 22°C and was gassed with 95% O_2 and 5% CO_2. Intracellular recording electrodes were filled with 2 M cesium acetate. In intracellular-injection experiments, L-Me-Arg (100 mM) was dissolved in cesium acetate. Whole-cell recordings were made in the single-electrode voltage-clamp mode (Axoclamp 2C) with 75 to 90% series resistance compensation. Whole-cell patch clamp internal solutions consisted of 100 mM cesium gluconate, 10 mM BAPTA, 5 mM $MgCl_2$, 2 mM adenosine triphosphate, 0.3 mM guanosine triphosphate, and 40 mM Hepes. Intracellular EPSP or whole-cell excitatory postsynaptic currents (EPSCs), measured in CA1 pyramidal cells, were evoked by stimulation of the Schaffer collateral–commissural afferents (4 min^{-1}). In dual recording experiments, we tested for the presence of synaptic or electrical connectivity by eliciting action potentials in one neuron and observing the response of the second neuron. We tested each pair for coupling at the beginning of each experiment and also tested at the conclusion of experiments where we were able to maintain the recordings for a sufficient period of time. LTP induction by pairing involved sustained depolarization of the pyramidal neuron by dc current injection in conjunction with low-frequency (1 Hz) stimulation of the test pathway for 30 to 45 s. LTP induction by

tetanus involved four high-frequency trains of stimulation (100 Hz for 1 s at 30-s intervals) delivered at the test intensity. Data were collected and analyzed with software written by us for this purpose under the Axobasic programming environment (Axon Instruments Incorporated, Foster City, CA). This software measured the amplitude or slope of the EPSP or EPSC. Statistical comparisons were made with the Student's *t* test, done on non-normalized data.

18. Ensemble average plots represent group means of each EPSP (or EPSC), across experiments, aligned with respect to the time of acquisition relative to the time of LTP induction by pairing. For each group of experiments, we included all the data that met the following criteria: (i) resting membrane potential of both neurons more negative than −60 mV and (ii) recordings of both cells held for at least 50 min after the induction of LTP. The group data in the ensemble averages and described in the text reflect all the data that fit these criteria. We did not exclude experiments where the paired neurons failed to exhibit LTP. For three experiments in which we had intended to impale neurons that were far apart, the biocytin data revealed that these neurons were in fact close (<300 μM). We thus switched these data to the nearby group.
19. We processed the slices for biocytin reaction with minor modifications of methods previously described [G. F. Tseng, I. Parada, D. A. Prince, *J. Neurosci. Methods* **37**, 121 (1991)]. To obtain a rough estimate of the distance between the synapses onto the paired and neighboring neurons, we measured the center to center intersomatic distance.
20. G. Lynch, J. Larson, S. Kelso, G. Barrionuevo, F. Schottler, *Nature* **305**, 719 (1983); R. C. Malenka, J. A. Kauer, R. S. Zucker, R. A. Nicoll, *Science* **242**, 81 (1988).
21. R. Malinow and J. P. Miller, *Nature* **320**, 529 (1986); S. R. Kelso, A. H. Ganong, T. H. Brown, *Proc. Natl. Acad. Sci. U.S.A.* **83**, 5326 (1986).
22. P. Sah, S. Hestrin, R. A. Nicoll, *Science* **246**, 815 (1989).
23. B. A. Ballyk and J. W. Goh, *J. Neurosci. Res.* **33**, 598 (1992); G. L. Collingridge, *Exp. Physiol.* **77**, 771 (1992).
24. P. R. Montague, J. A. Gally, G. M. Edelman, *Cereb. Cortex* **1**, 199 (1991).

25. We thank E. Schaible and I. Parada for technical assistance. We also thank J. Haley, T. Schwarz, and C. Shatz for comments on this manuscript.

19 July 1993; accepted 29 November 1993

TECHNICAL COMMENTS

Experimental Support for the "Hydrophobic Zipper" Hypothesis

In a recent report (*1*), we described the kinetics of folding of the all–β sheet protein interleukin-1β (IL-1β) with the use of nuclear magnetic resonance (NMR), far-ultraviolet dichroism, and fluorescence spectroscopy. The deuterium/hydrogen exchange quench flow experiments demonstrated that intermediates with a stable, hydrogen-bonded, secondary structure were only formed on the second time scale. Subsequent closer inspection of those parts of the IL-1β structure that are involved in these folding intermediates revealed clustering of hydrophobic residues, in particular, leucines. The five strands (Fig. 1) of the 12-stranded structure, which were detected in the NMR experiment (*1*), constitute the major site of early-forming hydrogen bonds. Within the symmetrical "trefoil" structure (*2*), they comprise hairpin 2 (strands 6 and 7) and parts of the adjacent barrel strands 5, 8, and 9. The locations of the major hydrophobic residues are also revealed (Fig. 1).

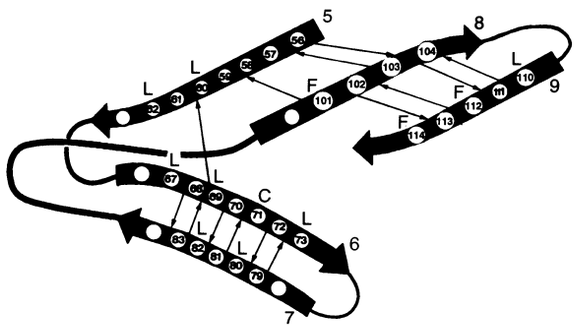

Fig. 1. Schematic picture of the early folding unit in IL-1β. Strands 5, 6, 7, and 8 represent the second of the three pseudosymmetric units of the "trefoil" fold, with strands 6 and 7 constituting the hairpin unit and strands 5 and 7 forming part of the β barrel. Early stable hydrogen bonds are indicated by arrows, and the identity of the important hydrophobic side chains is given by the one letter code.

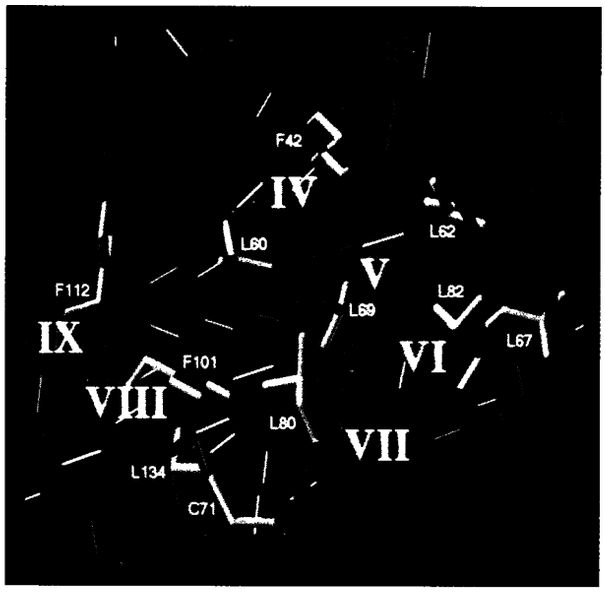

Fig. 2. Depiction of the "hydrophobic zipper" part of the IL-1β structure. The backbone (of N, C^{α}, and C atoms) is traced in red, and the side chains are shown in green. Also indicated is the residue number for the selected side chains and the numbering of the β strands (roman numerals). The structure of IL-1β is taken from (*4*) (PDB accession code 6I1B).

Our experimental data are similar to a recent theoretical model proposed by Dill *et al.* (*3*) that has been termed the "hydrophobic zipper" model of protein folding. In the initiation of folding, hydrophobic side chain pairs that are closely positioned in the sequence are brought together by a limited conformational search, with subsequent pairing of other pairs, one after another, like the zipping of a zipper. In IL-1β, the initial zipper would be made up from strands 6 and 7, with the other strands arranging around these. The location and distribution of hydrophobic side chains in this region of the protein structure add support to this notion (Fig. 2). The zipper-like arrangement of Leu^{67}, Leu^{82}, Leu^{69}, Leu^{80}, and Cys^{71}, running from right to left (Fig. 2), is most striking.

Angela M. Gronenborn
G. Marius Clore
Laboratory of Chemical Physics, National Institute of Diabetes and Digestive and Kidney Diseases, National Institutes of Health, Bethesda, MD 20892

REFERENCES

1. P. Varley *et al.*, *Science* **260**, 1110 (1993).
2. A. G. Murzin, A. M. Lesk, C. Chothia, *J. Mol. Biol.* **223**, 531 (1992).
3. K. A. Dill, K. M. Fiebig, H. S. Chan, *Proc. Natl. Acad. Sci. U.S.A.* **90**, 1942 (1993).
4. G. M. Clore, P. T. Wingfield, A. M. Gronenborn, *Biochemistry* **30**, 2315 (1991).

17 August 1993; accepted 20 October 1993